


RESEARCH ARTICLE

Transit passenger-oriented optimisation of arrival aircraft sequencing

S. Demirel 

Department of Air Traffic Control, Erzincan Binali Yildirim University, Erzincan, Turkey
Email: sdemirel@erzincan.edu.tr

Received: 17 July 2024; **Revised:** 14 September 2024; **Accepted:** 24 September 2024

Keywords: transit passenger; delay minimization; point merge; multi-objective optimization; emission analysis

Abstract

This study presents a model that aims to optimise the sequencing arrival aircraft around the terminal manoeuvring area (TMA). The model considers the transit passenger counts of these aircraft and employs the point merge at Sabiha Gokcen Airport. In this study, aircraft were categorised into two groups, namely ‘High or Low Transit Passenger (HTP/LTP)’. Subsequently, multi-objective models were employed to solve the test problems. Weighted sum scalarisation (WSS), conic scalarization (CS), and epsilon constraint (EC) models were utilised to increase robustness and their results were compared with a single-objective optimisation model. This approach aims to provide decision-makers with a variety of outcomes, thus expanding their options. Simultaneously, efforts are made within the model to allow aircraft with HTP counts to have minimal delays. Additionally, emission calculations were conducted to offer a critical perspective on the environmental implications, and the delay results of the multi-objective optimisation (MOO) models underwent statistical analysis.

Nomenclature

AIP	Aeronautical Information Publication
ALP	aircraft landing problem
ANOVA	analysis of variance
ASSP	aircraft sequencing and scheduling problem
CO	carbon monoxide
CS	conic scalarisation
EC	epsilon constraint
EUROCONTROL	European Organisation for the Safety of Air Navigation
H	heavy
HC	hydrocarbon
HTP	high-transit passengers
ICAO	International Civil Aviation Organization
LTP	low-transit passengers
M	medium
MOO	multi-objective optimisation
NO _x	nitrogen oxides
PMS	point merge system
SOO	single-objective optimisation
TMA	terminal manoeuvring area
WSS	weighted sum scalarisation

1.0 Introduction

Air transportation continues to become more popular among travelers due to it being a fast and safe mode of travel domestically and internationally. The demand for air travel has almost reached the level of 2019 when the last normal operations were managed before the COVID-19 pandemic. As stated in EUROCONTROL reports about current traffic levels over Europe, in September 2023, the number of flights in the European network was at 93% of 2019 levels [1]. As stated in the report, arrival and departure punctuality was 74.5/68.8%, respectively, in the first week of October 2023 and these percentages are lower than the 2019 and 2022 levels [1]. All these statistics show that the imbalance between capacity and demand is increasing. As a consequence of this, bottlenecks occur in the airspace, especially around the terminal manoeuvring area (TMA) and on the ground, which cause a decrease in arrival and departure punctuality. For this reason, efficient management of traffic flow around TMAs becomes more important to increase punctuality against the growing demand. One efficient way of managing traffic flow around TMA is the sequencing and scheduling of arrival aircraft. This effort contributes to mitigating noise, balancing capacity/demand, providing fuel management and optimising carbon emission efficiency. This problem is addressed in the aircraft landing problem (ALP), which is a subsection of the aircraft sequencing and scheduling problem (ASSP).

ALP has been the subject of extensive research in the literature. To access a comprehensive body of work regarding mathematical modeling to address ALP, see Refs [2, 3]. There are also some studies that have focused on some sequencing techniques around the TMA, such as the trombone method [4–6] and the point merge system (PMS) [7–15]. The trombone-shaped procedure involves parallel legs and multiple waypoints, which allow controllers to offer shortcuts based on the prevailing traffic conditions. On the other hand, the PMS includes sequencing legs that are equally spaced towards a merge point and controllers issue ‘direct-to’ instructions to aircraft on these legs once safe separation between aircraft has been. It proves advantageous in alleviating controllers’ workload, and it enhances the approach phase by facilitating continuous descent profiles [16]. The mentioned studies primarily focus on achieving the following objectives: optimising fuel efficiency, reducing delays and lowering the carbon emissions produced by aircraft [17].

Along with these studies, some research have focused on reducing passenger waiting time by planning a new flight without disrupting scheduled flights [18]. One such study was carried out with graphs, analytical equations and statistical parameters, where the researchers defined flight prioritisation according to the number of passengers with connecting flights [19]. In another study, the multi-objective gate assignment problem was handled based on arrival, departure, transit passengers walking distance and airline fairness [20]. This study focused on improving the ground movements of the passengers and tried to find an equal passenger walking distance for each airline. Another study aimed to minimise total passenger time and balance idle time at each gate, focusing on passenger satisfaction and service level [21]. In another study, aircraft prioritisation was carried out by employing algorithms to apply fleet delay apportionment and selective flight protection, these choices were presented to the airspace users to redistribute the delay across their fleet [22]. Within another research, the flight-gate assignment problem was examined to maximise the number of flights allocated to the lowest possible number of gates used by the flights to minimise the tension of transit passengers [23].

In this study, in contrast to the studies mentioned above which focus on transit passenger ground movements and optimisation models based on these passengers at ground level, the focus is on the relevant passengers in the arrival aircraft sequence around the TMA. It aims to present a different perspective from other studies therefore, in this research, each arrival flight was labeled high-transit passengers (HTP), or low-transit passengers (LTP), based on the average number of transit passengers for all flights scheduled at the reference operational time in the model. These two groups were then used in multi-objective optimisation (MOO) models (WSS, CS and EC) to manage the trade-offs between the objective functions. Finally, these outcomes were compared to the results of the single objective optimisation (SOO) model. Comparing MOO and SOO models helps us understand how different objective functions interact and trade off.

The criterion for labeling is distinctive from other criteria that were applied for prioritising flights specified in Sánchez, Etxebarria and Arranz, 2011. These researchers gave priority to flights by determining connecting flights that had a higher number of passengers or dividing ‘the number of passengers with connecting flights’ by ‘the total number of passengers’ and using the highest ratio. However, this study is based on a comparison between each flight’s total transit passenger count and the average transit passenger count of all flights scheduled at the reference operational time in the model. If the number of transit passengers on an aircraft is equal to or less than the average transit passenger count, the aircraft is labeled as LTP; otherwise, it is designated as HTP in the study. Furthermore, this study focuses on the whole TMA network and PMS system at the chosen airport, Istanbul Sabiha Gokcen (LTFJ). This airport is particularly busy and ranked 20th in average daily traffic over Europe in 2022. Furthermore, it has been observed that the TMA network and PMS system at LTFJ have not been previously studied using MOO models based on this approach in the literature and these aspects comprise the original components of this study together with the use of different labeling criteria.

To encapsulate the originality of the study, two key points can be emphasised:

- i. A comparative analysis of three MOO models and the SOO model assesses factors like delays and emissions, enhancing robustness of the study. The research pioneers the use of the MOO models for the entire TMA network at Istanbul Sabiha Gokcen Airport.
- ii. Unlike prior studies on ground-level issues, this research shifts the focus to arrival sequencing around TMA in terms of transit passengers. The study uniquely employs labeling criteria for grouping aircraft based on transit passengers, and it marks the first attempt to concentrate on the whole TMA structure and point merge at LTFJ, contributing significantly to the literature in methodology and practical application.

2.0 Problem statement and the point merge system at LTFJ

The study addresses the arrival aircraft sequencing problem around a TMA using a multi-objective modeling approach. One of the specific criteria chosen for this problem is the number of transit passengers on the aircraft. Furthermore, an objective function has been chosen to minimise HTP and LTP delays by considering the trade-offs between them and by employing three distinctive MOO models. In this study, to analyse the problem as described, aircraft were labeled based on their transit passenger counts, following the approach outlined previously. Furthermore, as this problem has been specifically examined within the context of Istanbul Sabiha Gökçen International Airport, the TMA routes and PMS are detailed as follows.

The PMS is actively used to sequence arrival traffic flow in LTFJ. While each directional aspect of the runway configuration incorporates a PMS, this research has specifically focused on the arrival routes associated with Runway 06. The analysis was predicated upon the predetermined route structure of the PMS at LTFJ, illustrated in Fig. 1. Seven entry points and eight air routes that pass through the sequencing legs exist in the TMA. Additionally, there are two sequencing legs that are vertically spaced (1,000 feet), and each connect to the same merge point for the PMS Runway 06 at LTFJ. The distance between merge point and runway is approximately 15 NM. Furthermore, the TMA has nine holding points as shown in the figure.

In this study, the routes and route connections used, route lengths, holding points and speeds within the route were employed exactly as stated in the Aeronautical Information Publication (AIP) published by the State Aviation Authority [24].

The potential conflicts at the entry points to the PMS were resolved based on delay considerations. It was assumed that aircraft could either wait at holding points within the TMA or receive a time margin over waypoints. In this study, these delay methods were referred to as ‘holding delay’ and ‘margin delay’ in the mathematical model. It is assumed that each waypoint for aircraft holding can be used at most

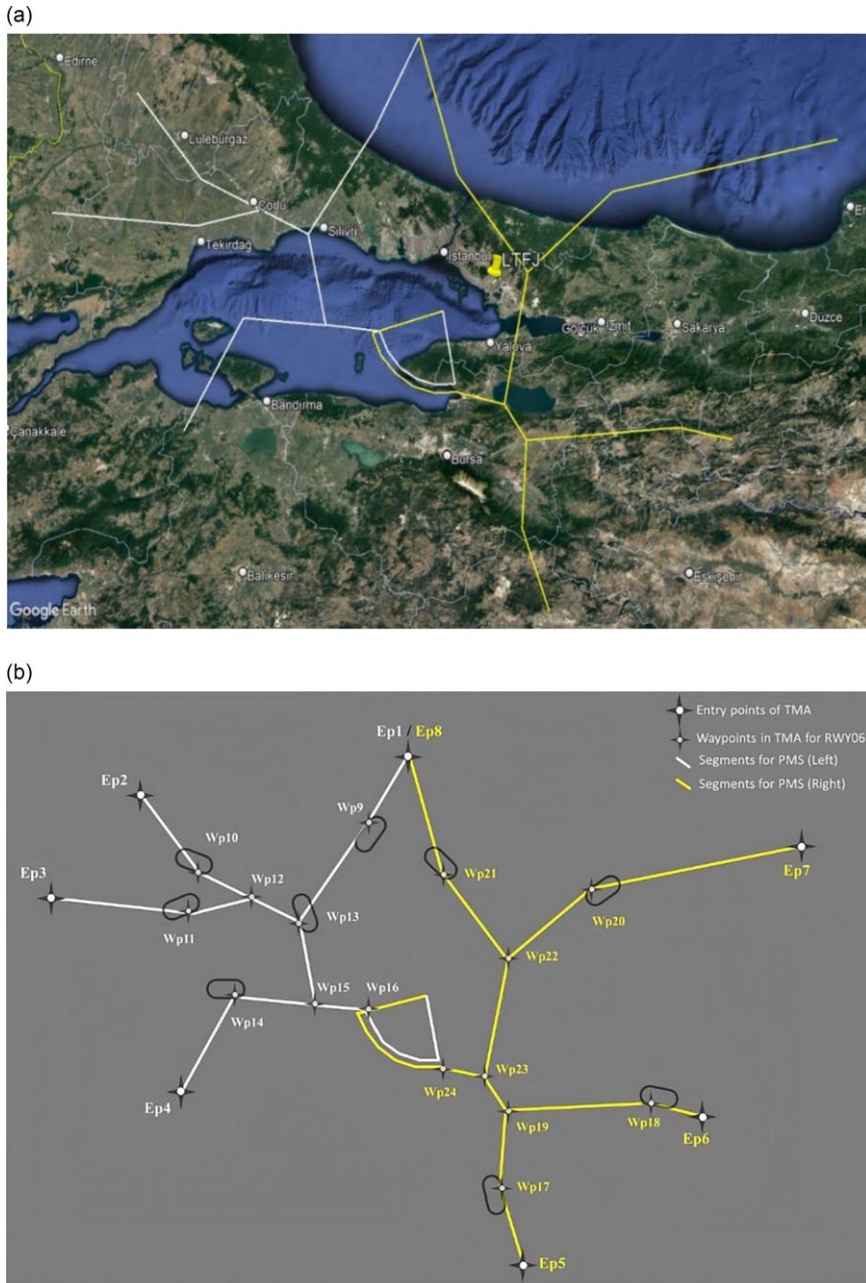


Figure 1. TMA route structures and PMS at LTFJ (a: TMA route structures illustrated on a Google Earth map; b: TMA routes and holding points).

twice to limit the maximum use of holding patterns. Additionally, vector and speed techniques can be applied by the controller to manage margin delays. Within the PMS, there are two sequencing legs. The distances from these legs to the merge point are equal, and aircraft flying on these legs turn towards the merge point with a ‘direct to’ instruction given by an air traffic controller. If traffic density permits, aircraft proceed directly to the merge point without flying on these legs. A constant speed is applied

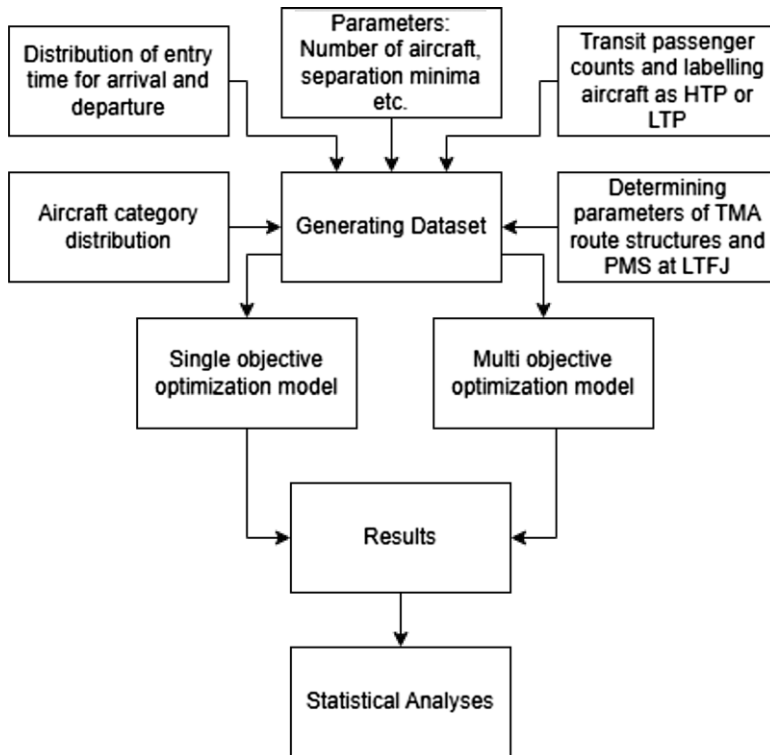


Figure 2. Conceptual model.

to all flights from the sequencing leg to the merge point. The model handles turn instruction from the sequencing leg to the merge point in a time-based manner by maintaining separation from the preceding aircraft while adhering to the length of the sequencing legs as defined in the AIP. Hence, the maximum flight duration on the legs was limited to ensure the model replicated the real conditions of the PMS at LTFJ. The time-based approach ensures more flexible control of traffic flow in this area. The conceptual and mathematical model of this study is explained in the following section.

3.0 Conceptual and mathematical model

3.1 Conceptual model

The conceptual model presented in Fig. 2 outlines the workflow. Initially, a dataset was generated with careful consideration of the parameters depicted in the figure. This facilitated the creation of both the dataset and test problems. Subsequently, the mathematical models for the SOO and MOO models were developed using the GAMS program. All result files were saved, and statistical analyses were conducted using the IBM SPSS 22 software.

3.2 Mathematical model

MOO models were developed to optimise the sequencing of arrival aircraft by considering the transit passenger numbers in each aircraft. Also, the SOO model was formed by combining two objectives into one equation.

Sets and Indices

I :	set of aircraft $(i, i1, i2) \in I \mid n(I) = 30$
O :	set of wake turbulence categories $(o1, o2) \in O \mid n(O) = 2$
P :	set of TMA entry points $p \in P \mid n(P) = 7$
W :	set of waypoints in the TMA $w \in W \mid n(W) = 24$

Parameters

α :	augmentation parameter (CS)
a_n :	a reference point (CS)
$avetransit$:	mean of the transit passenger count of all flights scheduled at the reference operational time (threshold value)
$cat(i)$:	wake turbulence category of each aircraft i
$csarr(o1,o2)$:	arrival separation (in second) between category $o1$ and $o2$ (at the merge point)
$csdep(o1,o2)$:	departure separation (in second) between category $o1$ and $o2$ (at departure)
ct :	coefficient for time conversion, from hour to seconds
$d(w1,w2)$:	distance matrix (in NM) between linked waypoints $w1$ and $w2$
$dist$:	distance between final approach fix and runway
$durmptfaf$:	flight duration (in second) between the merge point and final approach fix
$durseq$:	maximum flight duration (in second) on each sequence leg
$durseqmpt$:	flight duration (in second) between each sequence leg and the merge point
$ep(i)$:	TMA entry point of aircraft i
eps :	parameter of epsilon constraint (EC)
$et(i)$:	TMA entry time of arrival flight i ($fmode = 1$) or entry time of departure flight i at the holding point ($fmode = 2$)
$fmode(i)$:	flight status of flight i : 1 for arrival and 2 for departure
$h(w)$:	holding points at waypoint w : if there are holding pattern at waypoint w , it equals 1; otherwise equals 0
M :	large number
$maxgd$:	maximum duration of ground delays (in second) for each aircraft i on the ground
$maxhld$:	maximum number of holding patterns for each aircraft i at holding patterns
$maxhldcount$:	allowed maximum number that waypoints, $h(w) = 1$, can be used for holding pattern
$maxhlddur$:	maximum total duration (in second) for each aircraft i at holding patterns
$maxmctr$:	maximum number of instructions for aircraft i to apply margin delays
$maxmctrdur$:	maximum total margin delay (in second) of each aircraft i
$maxmd$:	allowed maximum margin delay (in second) for each aircraft i between linked waypoints $w1$ and $w2$
$minhd$:	minimum duration (in second) at a holding pattern if any exists.
$minmd$:	minimum margin delay (in second) if any exists
$pms(p)$:	PMS entry points
$r(p,w)$:	representing route of each aircraft according to the TMA entry point: equals 1 if a waypoint exists in the corresponding route; otherwise equals 0
$seg(w1,w2)$:	waypoint connection matrix: equals 1 if there is a link between two waypoints $w1$ and $w2$; otherwise equals 0
sep :	separation duration (in second) in TMA
$sep2$:	runway occupancy time (in second) in case an arrival aircraft uses the runway before departure

- sep3*: runway occupancy time (in second) in case a departure aircraft uses the runway before arrival
- transit(i)*: total number of transit passengers in each aircraft *i*
- v(w1,w2)*: speed matrix between linked waypoints *w1* and *w2*
- vfaf(o)*: final approach speed of each category *o*
- w*: weight parameters (MOO models)

Decision variables

- ad(i)*: total airborne delay of each aircraft *i*
- crmHLD(i)*: total number of holding patterns of each aircraft *i*
- crmMCTR(i)*: total number of instructions for applying margin delay to each aircraft *i*
- deptime(i)*: departure time of each aircraft *i* on the ground
- durseqleg(i)*: flight duration of each aircraft *i* on the sequence leg
- gd(i)*: ground delay of each departure aircraft *i*
- hd(i,w)*: holding delay of each aircraft *i* over waypoint *w*
- md(i,w1,w2)*: duration of margin delay between linked waypoints *w1* and *w2*
- mpt(i)*: time that aircraft *i* passes the merge point of the PMS
- n(i,w)*: number of holding patterns of aircraft *i* over waypoint *w*; *integer variable*
- t(i,w)*: time that aircraft *i* passes waypoint *w*
- tp(i)*: PMS entry time of each aircraft *i*
- x(i1,i2)*: (1); if arrival aircraft *i1* passes a waypoint before arrival aircraft *i2*, (0); otherwise
- y(i,w1,w2)*: (1); if aircraft *i* gets a margin delay instruction between linked waypoint *w1* and *w2*, (0); otherwise
- y2(i1,i2)*: (1) if arrival aircraft *i1* passes a merge point before arrival aircraft *i2*, (0); otherwise
- y3(i1,i2)*: (1) if arrival aircraft *i1* uses the runway before departure aircraft *i2*, (0); otherwise
- y4(i1,i2)*: (1) if departure aircraft *i1* uses the runway before departure aircraft *i2*, (0); otherwise

Separation minima between arrival-arrival and departure-departure are given in Table 1. All separation durations are given in seconds and were used in the mathematical model as parameters *csarr(o1,o2)* and *csdep(o1,o2)*.

Equations 1 and 2 present the objective functions in the mathematical model. Equation 1 focuses on minimising arrival delay of arrival flights that have more transit passengers than threshold value while Equation 2 consists of air and ground delay of all other aircraft. Equation 3 presents the combination of the objective functions for the SOO model. Equations 4–6 represent this combination for MOO models. For these formulations and detailed explanation, please refer to [25].

$$f_1 = \sum_{i|i \in I} ad_i, \tag{1}$$

$$transit_i > avetransit, fmode_i = 1$$

$$f_2 = \sum_{i1|i1 \in I} ad_{i1} + \sum_{i2|i2 \in I} gd_{i2}, \tag{2}$$

$$i1 \neq i2, transit_{i1} \leq avetransit, fmode_{i1} = 1, fmode_{i2} = 2$$

Table 1. Arrival and departure separation minima (sec.)

		Trailing		Trailing	
		Arrival – Arrival		Departure – Departure	
		Heavy	Medium	Heavy	Medium
Leading	Heavy	65	82	60	120
	Medium	49	49	60	60

$$\min_{SOO} \left(\sum_{n=1}^2 f_n \right) \tag{3}$$

$$\min_{WSS} \left(\sum_{n=1}^2 w_n * f_n \right) \tag{4}$$

$$\min_{CONIC} \left(\sum_{n=1}^2 w_n * (f_n - a_n) + \alpha * \sum_{n=1}^2 |f_n - a_n| \right) \tag{5}$$

$$\begin{aligned} \min_{EPSILON} (f_1) \\ \text{s.t. } f_2 \leq eps \end{aligned} \tag{6}$$

Constraint 7 calculates the entry times of the arrival aircraft into the TMA. Constraint 8 gives the passing times of each aircraft over waypoints by considering holding and margin delays. The calculation of the flight duration between two waypoints utilises the distance and speed information published in the AIP. Constraints 9 and 10 are responsible for monitoring the separations between aircraft flying towards the same waypoint.

$$\begin{aligned} t_{i,w} &= et_i, \\ w &= ep_i, fmode_i = 1, \forall i \in I, \forall w \in W \\ t_{i,w2} &= t_{i,w1} + (d_{w1,w2}/v_{w1,w2}) * ct + h_{w1} * hd_{i,w1} + md_{i,w1,w2}, \\ w1 \neq w2, r_{p,w1} &= 1, p = ep_i, seg_{w1,w2} = 1, fmode_i = 1, \forall i \in I, \\ \forall (w1, w2) \in W, \forall p \in P \end{aligned} \tag{8}$$

$$\begin{aligned} t_{i2,w} - t_{i1,w} &\geq sep - M * (1 - x_{i1,i2}), \\ i1 \neq i2, r_{p1,w} &= 1, r_{p2,w} = 1, p1 = ep_{i1}, p2 = ep_{i2}, fmode_{i1} = 1, fmode_{i2} = 1 \\ \forall (i1, i2) \in I, \forall w \in W, \forall (p1, p2) \in P \end{aligned} \tag{9}$$

$$t_{i1,w} - t_{i2,w} \geq sep - M * (x_{i1,i2}) ,$$

$$i1 \neq i2, r_{p1,w} = 1, r_{p2,w} = 1, p1 = ep_{i1}, p2 = ep_{i2}, fmode_{i1} = 1, fmode_{i2} = 1$$

$$\forall (i1, i2) \in I, \forall w \in W, \forall (p1, p2) \in P \tag{10}$$

Constraint 11 calculates the holding delay times for aircraft that enter a holding pattern. The division operation within this constraint ensures that, in the presence of a holding pattern, the delay time for each pattern is based on the *minhd* and its multiples. This formulation is employed to enhance both the smoothness of the holding pattern and its realism. Constraints 12 and 13 count holding instructions and constrain the total number of them, respectively. Constraint 14 limits the total holding pattern duration for each aircraft. Constraint 15 guarantees that each waypoint can only be used for a holding pattern up to the allowed maximum number. Constraint 16 includes a set of constraints to ensure that, if an aircraft is assumed to experience margin delay, *minmd* is guaranteed. If such a manoeuver is not required, the margin delay time for these aircraft is set to zero. Additionally, it limits the margin delay of each aircraft to a maximum duration of *maxmd* between waypoints. This set of constraints is presented in grouped form for readability. Constraints 17 and 18 count margin delay instructions and constrain the total number of them, respectively. Constraint 19 limits total margin delay for each aircraft.

$$n_{i,w} = (h_w * hd_{i,w}) / minhd ,$$

$$r_{p,w} = 1, p = ep_i, fmode_i = 1, \forall i \in I, \forall w \in W, \forall p \in P \tag{11}$$

$$crmHLD_i = \sum_{(w|w \in W)} \sum_{(p|p \in P)} n_{i,w} ,$$

$$r_{p,w} = 1, p = ep_i, fmode_i = 1, \forall i \in I \tag{12}$$

$$crmHLD_i \leq maxhld ,$$

$$fmode_i = 1, \forall i \in I \tag{13}$$

$$\sum_{(w|w \in W)} \sum_{(p|p \in P)} h_w * hd_{i,w} \leq maxhlddur ,$$

$$r_{p,w} = 1, p = ep_i, fmode_i = 1, \forall i \in I \tag{14}$$

$$\sum_{(i|i \in I)} \sum_{(p|p \in P)} n_{i,w} \leq maxhldcount ,$$

$$r_{p,w} = 1, p = ep_i, fmode_i = 1, h_w = 1, \forall w \in W \tag{15}$$

$$md_{i,w1,w2} \geq 0 - M * y_{i,w1,w2}$$

$$md_{i,w1,w2} \leq 0 + M * y_{i,w1,w2}$$

$$md_{i,w1,w2} \geq minmd - M * (1 - y_{i,w1,w2})$$

$$md_{i,w1,w2} \leq maxmd ,$$

$$w1 \neq w2, r_{p,w1} = 1, p = ep_i, seg_{w1,w2} = 1, fmode_i = 1, \forall i \in I, \forall (w1, w2) \in W, \forall p \in P \quad (16)$$

$$crmMCTR_i = \sum_{(w1|w1 \in W)} \sum_{(w2|w2 \in W)} \sum_{(p|p \in P)} y_{i,w1,w2} ,$$

$$w1 \neq w2, r_{p,w1} = 1, p = ep_i, seg_{w1,w2} = 1, fmode_i = 1, \forall i \in I \quad (17)$$

$$crmMCTR_i \leq maxmctr ,$$

$$fmode_i = 1, \forall i \in I \quad (18)$$

$$\sum_{(w1|w1 \in W)} \sum_{(w2|w2 \in W)} \sum_{(p|p \in P)} md_{i,w1,w2} \leq maxmctrdur ,$$

$$w1 \neq w2, r_{p,w1} = 1, p = ep_i, seg_{w1,w2} = 1, fmode_i = 1, \forall i \in I \quad (19)$$

Constraint 20 provides the entry times of the aircraft into the PMS. Constraint 21 calculates the passing time for each aircraft over the merge point. This calculation considers the time aircraft spend on the sequencing leg and the flight duration from the sequencing leg to the merge point. Constraints 22 and 23 ensure that the separation between consecutive arrival aircraft adheres to the time intervals specified in Table 1. Constraint 24 constrains the maximum flight duration on the sequencing legs.

$$tp_i = t_{i,w} ,$$

$$w = pms_p, p = ep_i, fmode_i = 1, \forall i \in I, \forall w \in W, \forall p \in P \quad (20)$$

$$mpt_i = tp_i + durseqmpt + durseqleg_i ,$$

$$fmode_i = 1, \forall i \in I \quad (21)$$

$$mpt_{i2} - mpt_{i1} \geq csarr_{o1,o2} - M * (1 - y2_{i1,i2}) ,$$

$$i1 \neq i2, o1 = cat_{i1}, o2 = cat_{i2}, fmode_{i1} = 1, fmode_{i2} = 1, \forall (i1, i2) \in I, \forall (o1, o2) \in O \quad (22)$$

$$mpt_{i1} - mpt_{i2} \geq csarr_{o1,o2} - M * y2_{i1,i2} ,$$

$$i1 \neq i2, o1 = cat_{i2}, o2 = cat_{i1}, fmode_{i1} = 1, fmode_{i2} = 1, \forall (i1, i2) \in I, \forall (o1, o2) \in O \quad (23)$$

$$durseqleg_i \leq durseq ,$$

$$fmode_i = 1, \forall i \in I \quad (24)$$

Constraint 25 calculates the departure times of aircraft on the ground by considering the ground delay time. Constraints 26 and 27 are used to ensure the separations between landing and departing aircraft by sep2 (60 sec.) and sep3 (75 sec.), respectively. In these equations, ICAO Doc 8168 was used to determine the final approach speed (v_{faf_o}) for each aircraft category [26]. An approach speed of 200 knots is applied between the initial and final approach fix. Additionally, for heavy traffic, a final approach speed of 150 knots is applied while for medium traffic, a speed of 130 knots is used. Constraints 28 and 29 ensure that the separation between consecutive departure aircraft adheres to the time intervals specified in Table 1. Constraint 30 constrains the maximum delay duration on the ground. Constraint 31 calculates the total airborne delay duration for each aircraft. This calculation considers the time spent on the sequencing legs, holding delays and margin delays. Constraint 32 presents the sign constraints of the model.

$$\begin{aligned}
 deptime_i &= et_i + gd_i \\
 fmode_i &= 2, \forall i \in I
 \end{aligned} \tag{25}$$

$$\begin{aligned}
 deptime_{i_2} - \left(mpt_{i_1} + durmptfaf + \left(\frac{dist}{v_{faf_o}} * ct \right) \right) &\geq sep2 - M * (1 - y_{3_{i_1,i_2}}), \\
 i_1 \neq i_2, fmode_{i_1} = 1, fmode_{i_2} = 2, \forall (i_1, i_2) &\in I
 \end{aligned} \tag{26}$$

$$\begin{aligned}
 \left(mpt_{i_1} + durmptfaf + \left(\frac{dist}{v_{faf_o}} * ct \right) \right) - deptime_{i_2} &\geq sep3 - M * y_{3_{i_1,i_2}}, \\
 i_1 \neq i_2, fmode_{i_1} = 1, fmode_{i_2} = 2, \forall (i_1, i_2) &\in I
 \end{aligned} \tag{27}$$

$$\begin{aligned}
 deptime_{i_2} - deptime_{i_1} &\geq csdep_{o_1,o_2} - M * (1 - y_{4_{i_1,i_2}}), \\
 i_1 \neq i_2, o_1 = cat_{i_1}, o_2 = cat_{i_2}, fmode_{i_1} = 2, fmode_{i_2} = 2, \forall (i_1, i_2) &\in I, \forall (o_1, o_2) \in O
 \end{aligned} \tag{28}$$

$$\begin{aligned}
 deptime_{i_1} - deptime_{i_2} &\geq csdep_{o_1,o_2} - M * y_{4_{i_1,i_2}}, \\
 i_1 \neq i_2, o_1 = cat_{i_2}, o_2 = cat_{i_1}, fmode_{i_1} = 2, fmode_{i_2} = 2, \forall (i_1, i_2) &\in I, \forall (o_1, o_2) \in O
 \end{aligned} \tag{29}$$

$$\begin{aligned}
 gd_i &\leq maxgd, \\
 fmode_i &= 2, \forall i \in I
 \end{aligned} \tag{30}$$

$$\begin{aligned}
 ad_i &= durseqleg_i + \sum_{(w1|w1 \in W)} \sum_{(w2|w2 \in W)} \sum_{(p|p \in P)} md_{i,w1,w2} + \sum_{(w|w \in W)} \sum_{(p|p \in P)} h_w * hd_{i,w} \\
 w1 \neq w2, r_{p,w1} = 1, r_{p,w} = 1, p = ep_i, seg_{w1,w2} = 1, fmode_i &= 1, \forall i \in I
 \end{aligned} \tag{31}$$

$$\begin{aligned}
 x_{i_1,i_2}, y_{i,w1,w2}, y_{2_{i_1,i_2}}, y_{3_{i_1,i_2}}, y_{4_{i_1,i_2}} &\in \{0, 1\} \\
 n_{i,w}, crmHLD_i, crmMCTR_i &\in Z^+ \\
 \text{all remaining variables} &\geq 0
 \end{aligned} \tag{32}$$

4.0 Scenarios and results

The analysis of the study focused on the heavy (H) and medium (M) categories, with these two categories distributed as 50H-50M, 70H-30M, 30H-70M and 100M. The last distribution was determined as regarding aircraft characteristics in LTFJ. Each distribution was tested with three different sub-problems that have different number of transit passengers. In these problems, the expected maximum number of transit passengers that each aircraft could accommodate was calculated by multiplying the number of passengers on the aircraft, the percentage of transit passengers, and the probability of this percentage occurring. The expected maximum number of transit passengers was determined basically by multiplying the total number of passengers, which was 300 for H and 189 for M category, by the specified percentages of transit passengers which were set at 30% and 50%, and the realisation probabilities of 0.7 and 0.3. These values were employed specifically for the analyses in this study. These values were chosen arbitrarily, ensuring consistency by using the same values across all tests. Although this approach may raise concerns about potential bias, it was implemented to maintain uniformity and facilitate comparability across experiments. The assignment of these probabilities to the percentages was based on the consideration that a lower percentage of transit passengers had a higher likelihood of occurrence in real operations. The percentages and probabilities were used uniformly for all aircraft only for calculating the expected maximum number of transit passengers. The highest passenger count resulting from these calculations defined the maximum number of transit passengers parameter for the respective aircraft. Finally, transit passenger counts were assigned randomly within the range of zero to the maximum number for each aircraft.

In total, each MOO model was tested with four different aircraft category distributions, and within each distribution, three different sub-problems, each one with a varied number of transit passengers, were tested. This resulted in the creation of 12 different test problems for each model, and each test problem was tested with 50 iterations for all three objective function formulations. Consequently, a total of 1800 ($12 \times 3 \times 50$) distinct result data were generated, and these results were consolidated in Excel for post-optimisation analyses. This experiment was developed to assess the model's responses and efficiency in the face of changing transit passenger counts. The entry times of aircraft were distributed exponentially, and the model was tested with 30 aircraft (20 arrivals and 10 departures) in a one-hour time window.

The rest of this section consists of three parts which are based on the optimisation and statistical results. The first presents the numerical results of MOO and SOO models, the comparison between them, and the pareto optimal solutions. The second gives the comprehensive analysis of the outcomes in terms of emission metrics. The last part presents the statistical analysis and the evaluation of the results of MOO in terms of statistical significance.

4.1 Numerical results

The comparison between the average delay of HTP and LTP flights is shown in Table 2. It presents the average total delays, in seconds, for flights labeled as HTP and LTP in the results of three different MOO models and the SOO model. There are 50 iterations for each MOO model, constituting a total of three distinct sub-problems across these 50 iterations. To elucidate, consider the model WSS-50H-50M-1: it undergoes 50 iterations to obtain Pareto-optimal points. Additionally, there exist two more sub-problems denoted as WSS-50H-50M-2 and WSS-50H-50M-3. Consequently, the average delay is computed by aggregating all delays for HTP and LTP, and subsequently dividing this cumulative value by 150 (representing the product of 50 iterations and 3 sub-problems). This calculation serves to portray the overall performance of each model across different sub-problems. To enhance clarity, direct representation is preferred over percentages in this table, and single objective results were separated as HTP and LTP as well after obtaining the results from the model.

When looking at delay times on an average basis, it is evident that HTP flights under the category distribution of 30–70 exhibited the lowest delay times in the CS model. It can be observed that this model has proven to be more effective in reducing delay times for HTP flights compared to other models.

Table 2. Average delays of HTP and LTP flights (sec.)

Model	50H-50M		70H-30M		30H-70M		100M	
	HTP delay	LTP delay	HTP delay	LTP delay	HTP delay	LTP delay	HTP delay	LTP delay
WSS	160.99	351.41	225.78	288.80	98.04	344.88	125.28	170.44
CS	124.22	471.87	151.75	350.94	79.08	445.95	109.49	182.70
EC	117.67	521.38	183.81	378.02	102.27	469.61	97.13	311.45
SOO	161.14	327.61	202.16	265.61	102.15	317.90	131.50	139.25

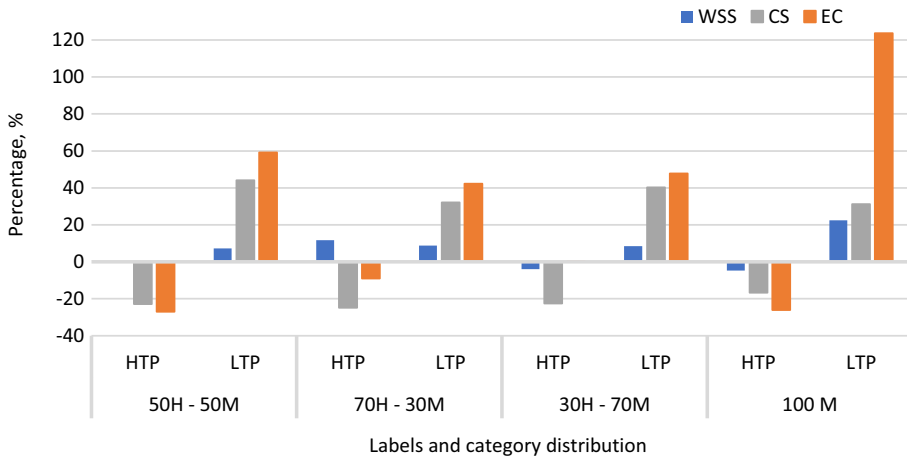


Figure 3. Comparison of models in terms of HTP and LTP delays.

However, due to the trade-off approach, it has affected the delay times for LTP aircraft, but it has not significantly deviated from the results obtained from the other models. The SOO model has the lowest LTP delay time, at 139.25 seconds, in the 100M. However, its HTP delay time is higher compared to CS, WSS and EC models in the same category distribution. Figure 3 provides a comparison between MOO models and the SOO model based on the average delay times given in Table 2.

The percentages provided in Fig. 3 encompass the comparison of the results between the SOO model and the respective MOO models based on the averages for the given category distributions. Positive values indicate that the SOO model produced better results while negative values indicate that the corresponding MOO model achieved superior results. As can be observed from the figure, the CS model outperformed the SOO model by -22.91% , -24.93% , -22.58% and -16.73% for 50H-50M, 70H-30M, 30H-70M and 100M category distribution on HTP delay, respectively. On the other hand, when considering the LTP delay times, the WSS model yielded better results when compared to the other MOO models across all categories. But, for the same delay, the SOO model achieved superior results compared to the MOO models across all category distributions. For 100M distribution, EC delivered the best result for HTP delay among the MOO models while the opposite was true for the LTP delay.

In Fig. 4, average delay times for each distribution are provided for the MOO and the SOO models. As evident from this figure, the model has scarcely utilised holding delays in any solution model or category distribution. In the 50-50 distribution, while the SOO model and WSS model nearly equally employ margin delays, the CS model proves more efficient for sequence delay in the same distribution. In the 70-30 distribution, the CS model continues to yield better results for sequence delay, while for ground delay, the SOO model exhibits a slight but favourable differentiation from the others. For margin delay, the WSS model achieved superior result compared to the MOO models in the 30-70 distribution.

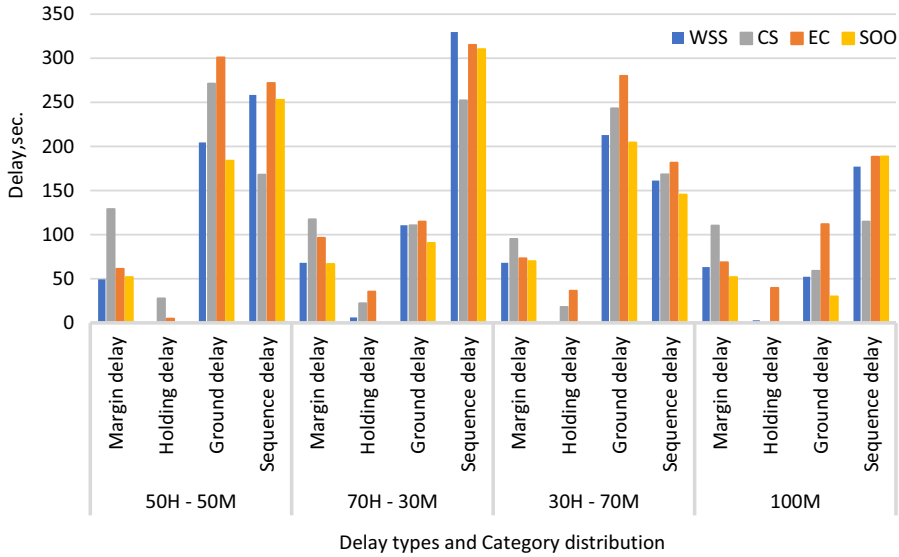


Figure 4. Type of delays.

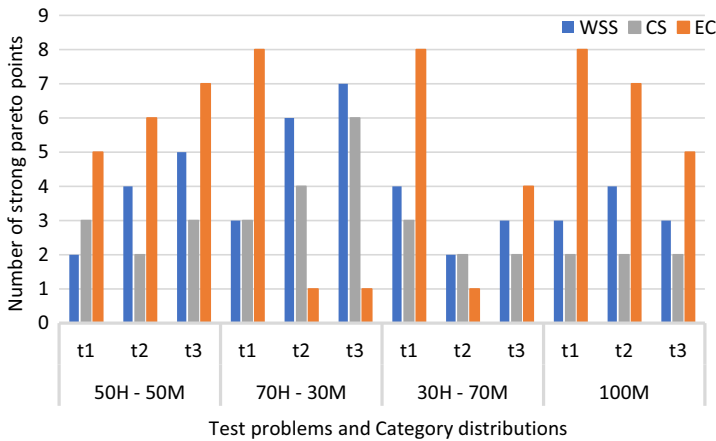


Figure 5. Total number of pareto optimal points.

This model also outperforms the other MOO models in terms of holding delays across all category distributions. In the 100M distribution, ground delay was needed less compared to the others. The main reason for this is that the required separation time for medium traffics is shorter than for mixed traffics.

Multi-objective optimisation inherently provides decision-makers with various solutions, catering to the complexities of conflicting objectives. The number of pareto-optimal points obtained from each MOO model is presented in Fig. 5. The number of pareto-optimal points is provided for each distribution in the figure, along with their sub-problems (t1-t3), for each MOO model. These numbers were found by counting the strong pareto dominances obtained for each outcome. The EC model generally produced a greater number of pareto results than the other models.

Figure 6 depicts the pareto-optimal fronts generated by the MOO models for the results of a randomly selected test problem in this study. In this figure, the discrepancy in the number of pareto-optimal points among the MOO models may indicate the effectiveness of each model in exploring the solution space.

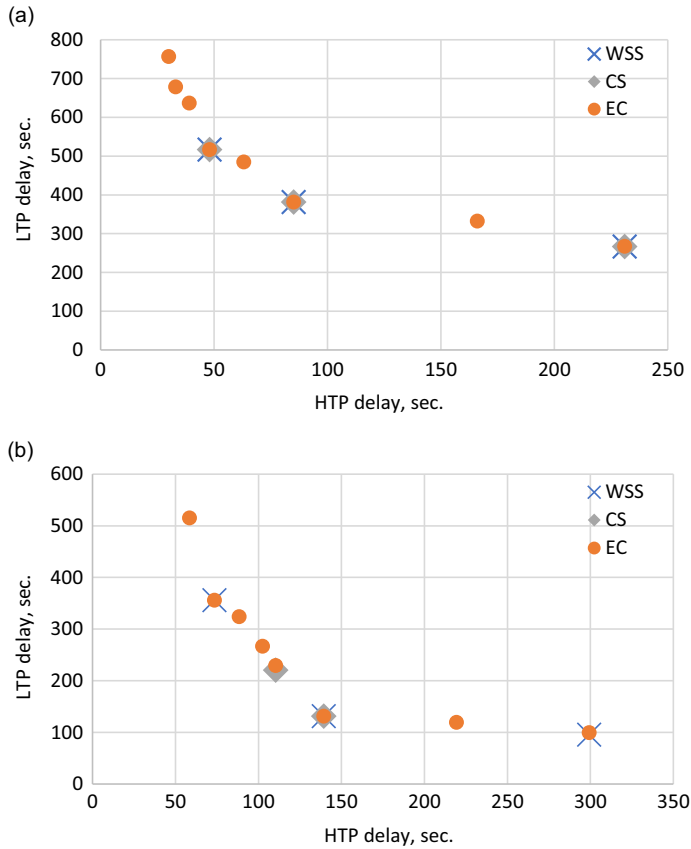


Figure 6. Pareto optimal fronts of each MOO model (a: 70H-30M; test no: 1, b: 100M; test no: 1).

Specifically, the EC model, with 8 pareto-optimal points, seems to be the most effective in finding various trade-off solutions compared to the other models for the related category distribution and test problem. The greater number of pareto-optimal points in the EC model could suggest that it provides a wider range of feasible solutions that balance the competing objectives, which can be valuable when decision-makers seek a variety of options.

4.2 Emission insights in optimisation results

In the context of optimising the solution, the primary goal lies in managing trade-offs between the objective functions which are related to aircraft delay in this study. Despite the absence of a direct optimisation goal for emissions, their quantification provides a critical insight regarding the environmental implications of the solutions.

The formula, Equation 33 [27], provided below has been utilised for the analysis of emission values within this study. TIM, FF, EI, Ne and E stand for time in mode, fuel flow, emission index, the number of engines and total emissions of each pollutant, respectively. The indices i, j and k are used to denote the pollutant, aircraft and aircraft operation mode, respectively. The FF and EI values of each aircraft type used in the study can be seen in Table 3 [28]. In the absence of a distinct holding pattern index in the database, the APP index was applied for emission calculations during the holding phase if any pattern exists. These values were employed uniformly for each test problems.

Table 3. Emission index and fuel flow coefficients

Aircraft	HC EI	HC EI	CO EI	CO EI	NOx EI	NOx EI	Fuel Flow	Fuel Flow
	App (g/kg)	Idle (g/kg)	App (g/kg)	Idle (g/kg)	App (g/kg)	Idle (g/kg)	App (kg/sec)	Idle (kg/sec)
A342-H	0.07	5	1.4	30.93	10.67	4.28	0.386	0.124
B738-M	0.1	2.4	2.2	22	10.1	4.4	0.316	0.109

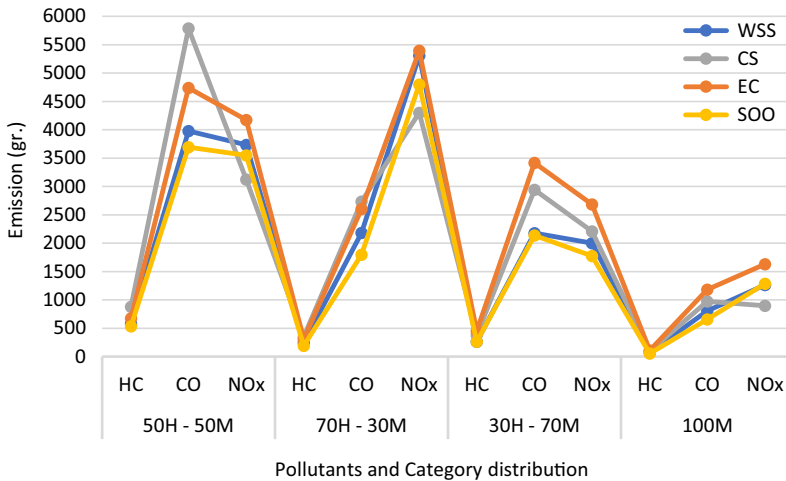


Figure 7. Emission values for HC, CO and NOx.

All emission calculations have been conducted based on holding patterns, margin delay instructions, time spent on the sequencing leg and ground delays, excluding emission calculations for routine flight phases for each aircraft. The primary reason for this is to integrate emission calculations more cohesively with the objective functions of the research. This approach aims to align the calculation methodology with the overarching goal of the study.

$$E_{ij} = \sum TIM_{jk} * FF_{jk} * EI_{ijk} * Ne_j \tag{33}$$

Emission values calculated based on the MOO and the SOO models are represented in Fig. 7. In the figure, average emission values for HC, CO and NOx are provided for each MOO and the SOO model. While models generally exhibit relatively little variation for HC, distinctions are evident for CO and NOx emissions. In a 50H-50M distribution, the WSS model may be considered better choice for CO among the MOO models, whereas for NOx in the same distribution, the CS model yields a lower emission value. In a 70H-30M distribution, the SOO model achieves the best values for CO while the CS model once again attains superior emission values for NOx compared to the other models. However, when examining the 30H-70M distribution, the dynamics shift slightly. While the WSS model is more effective for CO among the MOO models, the SOO model yields superior results for the NOx pollutant. In the 100M distribution, the SOO and CS delivered better results than the others for the CO and the NOx pollutant, respectively.

4.3 Statistical analysis

Statistical analyses were carried out to compare the differences between the means of the MOO models' results. In this study, three distinct MOO models constitute the independent variables while the variables HTP and LTP delay serve as the dependent variables. The objective is to ascertain whether these

Table 4. ANOVA and Welch test

Category	Dependent variable	Sig.		
		Levene statistic	ANOVA	Welch
50H-50M	HTP delay	.000	–	.000*
	LTP delay	.000	–	.000*
70H-30M	HTP delay	.000	–	.000*
	LTP delay	.859	.000*	–
30H-70M	HTP delay	.028	–	.012*
	LTP delay	.000	–	.000*
100M	HTP delay	.324	.010*	–
	LTP delay	.000	–	.000*

three different models employed for problem-solving exhibit statistically significant differences from one another. The results of the three test problems for each category distribution were combined and subjected to statistical testing according to their respective distributions. To decide on the appropriate statistical method, an initial step involved testing whether the variables (HTP and LTP) exhibited a normal distribution. This test was conducted using IBM SPSS 22. Prior to the analysis, missing data were examined, and outliers were identified and excluded. Subsequently, a test for normality was performed with the interpretation relying on the Skewness and Kurtosis values. When these values fall within the range of -1 to $+1$, it is considered that the variable values follow at least approximately normal distribution and some parametric tests such as the one-way ANOVA are quite robust to show meaningful results under this condition [29].

As a result of the normality test, it was seen that the Skewness and Kurtosis values for each analysis were located between -1 and $+1$. Hence, it was assumed that the dependent variables in each analysis followed a normal distribution, allowing for the applicability of parametric tests to compare the mean values of the dependent variables. With both the assumption of normality and the presence of four independent variables, the choice was made to employ the one-way ANOVA test for the analyses. This test is a statistical technique employed to assess the differences among the means of three or more groups [30]. It is utilised to determine whether there are significant variations in the dependent variable concerning the categorical independent variable. The results of this test is given in Table 4.

In accordance with the Levene statistic, it is observed that the variance homogeneity assumption ($p_{value} \geq .05$) is met for the LTP delay in the 70H-30M distribution and HTP delay in the 100M distribution, whereas it is not satisfied for the other distributions. Consequently, the ANOVA test has been employed for the group with homogeneous variances while the Welch test has been utilised for the remaining groups. All results marked with an asterisk (*) indicate that the MOO models differ from each other in a statistically significant way ($p_{value} < .05$) in corresponding dependent variables. Furthermore, post hoc tests were conducted.

The Scheffe test was employed as a post hoc analysis in cases where the variance homogeneity assumption ($p_{value} \geq .05$) was met in the Levene statistic. On the contrary, the Games-Howell test was applied in other instances. The results of this are summarised in Table 5, highlighting only the statistically significant differences. For the mean difference values calculated positively according to the (I–J) operation in the Mean Difference column of Table 5, the mean delay values of variables in column I are greater than the mean values of the variables in column J.

Upon examining the significant differences, it can be generally stated that the WSS and CS models provided lower delay values than the EC model. As an example, the largest difference occurred in the dependent variable LTP delay for the 70H-30M distribution, specifically between EC and WSS. In this case, the average LTP delay value obtained with EC is 288.02 seconds higher than that obtained with WSS. The smallest difference (13.14 seconds) was observed in the HTP delay variable for the 30H-70M

Table 5. *Post hoc tests*

Category Distribution	Dependent variables	I (Independent variables)	J (Independent variables)	Mean Difference (I-J)	Sig.
50H-50M	HTP delay	WSS	CS	34.99	.000
		WSS	EC	49.06	.000
	LTP delay	CS	WSS	119.91	.000
		EC	WSS	177.20	.000
		EC	CS	57.28	.001
		EC	CS	57.28	.001
70H-30M	HTP delay	WSS	CS	74.03	.000
		EC	CS	116.44	.000
	LTP delay	CS	WSS	62.14	.006
		EC	WSS	288.02	.000
		EC	CS	225.88	.000
		EC	CS	225.88	.000
30H-70M	HTP delay	WSS	CS	13.14	.015
	LTP delay	CS	WSS	98.39	.000
		EC	WSS	83.32	.000
100M	HTP delay	WSS	EC	28.15	.010
	LTP delay	EC	WSS	141.01	.000
		EC	CS	129.60	.000

distribution, again between WSS and CS. In this case, the average value obtained with WSS. is higher than that obtained with CS.

In conclusion, the one-way ANOVA and post hoc tests conducted in this section provided valuable insights into the differences and trends within the results. The results have elucidated the significant differences between the MOO models as revealed by the post hoc comparisons in Table 5.

5.0 Conclusion and discussion

Research in the field of aircraft sequencing has primarily concentrated on optimising various aspects of aircraft operations, such as fuel efficiency, delay minimisation or runway allocation. However, this study takes an approach by introducing a novel dimension – the integration of transit passengers into the arrival aircraft sequencing model within a TMA.

This research fundamentally differs from previous studies by focusing on arrival sequencing as regarding transit passenger counts in arrivals. To address this, the study categorises arrival flights into two groups: high-transit passengers (HTP) and low-transit passengers (LTP).

To manage aircraft sequencing within the TMA by considering trade-offs between objectives effectively, the study employs MOO models. These models include WSS, CS and EC. Each of these models has been carefully tailored to address specific aspects of optimising aircraft sequencing. The results obtained from the MOO models were systematically compared both among themselves and with the results derived from the SOO model. This comparative analysis serves to offer valuable insights into the trade-offs existing between the various objectives and highlights the potential advantages of the proposed approach.

The use of MOO, with the flexibility to assign weights, has a significant advantage. These weights were selected to ensure that each MOO model had an equal number of iterations, facilitating a homogeneous comparison between the models. Decision-makers can manage the trade-offs between aircraft labeled as HTP or LTP according to their objectives and preferences. The ability to adjust the weighting

of the objective functions allows decision-makers to make more informed choices based on their operational priorities. For instance, during peak transit passenger seasons, prioritising HTP by considering trade-offs between objectives might be more beneficial.

Effective communication and coordination are crucial for aligning this approach with the operational strategies of airlines and airports. Achieving a consensus among stakeholders on the weighting scheme can be challenging. The accuracy of data regarding transit passenger counts is paramount as errors in data can lead to suboptimal decisions and thus ensuring data accuracy is essential for the approach's success.

The approach employed in this study allows for a more customised method of air traffic management based on the characteristics of passengers carried by aircraft. Furthermore, the results obtained through the application of the MOO models in this study are adaptable according to the operational objectives of decision-makers. Hence, the model and features are generalisable and applicable for different types of objective functions and airports. As a result, these findings serve as a guide for enhancing efficiency and passenger experience in air transportation. The subsequent step involves integrating this approach into a machine learning technique to harmonise it with a predictive effort.

Competing interests. There is no potential conflict of interest was reported by the author.

References

- [1] EUROCONTROL, *European Aviation Overview (02-08 Oct 2023)*, Publisher: EUROCONTROL.
- [2] Bennell, J.A., Mesgarpour, M. & Potts, C.N. (2013). Airport runway scheduling, *Annals of Operations Research*, **204**, (1), pp. 249–270. <https://doi.org/10.1007/S10479-012-1268-1>
- [3] Sama M., D'ariano A., D'ariano P. & Pacciarelli D. (2017). Scheduling models for optimal aircraft traffic control at busy airports: tardiness, priorities, equity and violations considerations, *Omega*, **67**, pp. 81–98.
- [4] Dalmau, R., Alenka, J. & Prats, X. (2017). Combining the assignment of pre-defined routes and RTAs to sequence and merge arrival traffic, 17th AIAA Aviation Technology, Integration, and Operations Conference, 1–12.
- [5] Sáez, R., Dalmau, R. & Prats, X. (2018). Optimal assignment of 4D close-loop instructions to enable CDOs in dense TMAs, AIAA/IEEE Digital Avionics Systems Conference – Proceedings, <https://doi.org/10.1109/DASC.2018.8569597>
- [6] Sáez, R., Prats, X., Polishchuk, T. & Polishchuk, V. (2020). Traffic synchronization in terminal airspace to enable continuous descent operations in trombone sequencing and merging procedures: an implementation study for Frankfurt airport, *Transportation Research Part C*, **121**, pp. 102875. <https://doi.org/10.1016/j.trc.2020.102875>
- [7] Boursier, L., Favennec, B., Hoffman, E., Trzmiel, A., Vergne, F. & Zeghal, K. (2007). Merging arrival flows without heading instructions, *Proceedings of the 7th USA/Europe Air Traffic Management Research and Development Seminar*, ATM 2007, pp. 1–8.
- [8] Liang, M., Delahaye, D. & Maréchal, P. (2017). Integrated sequencing and merging aircraft to parallel runways with automated conflict resolution and advanced avionics capabilities, *Transportation Research Part C*, **85**, pp. 268–291. <https://doi.org/10.1016/j.trc.2017.09.012>
- [9] Liang, M., Delahaye, D. & Marechal, P. (2018). Conflict-free arrival and departure trajectory planning for parallel runway with advanced point-merge system, *Transportation Research Part C*, **95**, pp. 207–227. <https://doi.org/10.1016/j.trc.2018.07.006>
- [10] Sahin, O., Usanmaz, O. & Turgut, E.T. (2018). An assessment of flight efficiency based on the point merge system at metroplex airports, *Aircraft Engineering and Aerospace Technology*, **90**, (1), pp. 1–10. <https://doi.org/10.1108/AEAT-06-2016-0097>
- [11] Cecen, R.K. (2021). Multi-objective TMA management optimization using the point merge system, *Aircraft Engineering and Aerospace Technology*, **93**, (1), pp. 15–24, <https://doi.org/10.1108/AEAT-09-2019-0181>
- [12] Cecen, R.K. (2022). A path stretching model for effective terminal airspace management, *International Journal of Aeronautical and Space Sciences*, **23**, pp. 1043–1052. <https://doi.org/10.1007/s42405-022-00486-z>
- [13] Cecen, R.K. (2022a). The fuel consumption impact of the turning point location for the point merge system, *International Journal of Sustainable Aviation*, **8**, (1), pp. 75–90. <https://doi.org/10.1504/IJSA.2022.120612>
- [14] Cecen, R.K., Saraç, T. and Çetek, C. (2022b). Emission and flight time optimization model for aircraft landing problem, *Transportation Research Record: Journal of the Transportation Research Board*, **2677**, (2). <https://doi.org/10.1177/03611981221108398>
- [15] Dönmez, K., Çetek, C., & Kaya, O. (2022). Aircraft sequencing and scheduling in parallel-point merge systems for multiple parallel runways. *Transportation Research Record*, **2676**(3), pp. 108–124.
- [16] Aydoğan, E., & Çetek, C. (2018). Point merge concept for en route air traffic flow management. *Journal of Aircraft*, **55**(6), pp. 2203–2216.
- [17] Demirel, S. (2023). Comparison of RECAT-EU and ICAO wake turbulence category on the Point Merge System. *The Aeronautical Journal*, pp. 1623–1637. <https://doi.org/10.1017/aer.2023.17>

- [18] Taçoğlu, M.T., & Örnek, M.A. (2023). Intelligent Flight Scheduling for Transit Passengers by Introducing New Flights in Hub-and-Spoke Network. In International Conference on Intelligent and Fuzzy Systems (pp. 700–708). Cham: Springer Nature Switzerland.
- [19] Sánchez, M., Etxebarria, I., & Arranz, A. (2011). A. Dynamic Approaches from Complexity to Manage the Air Transport Network. First SESAR Innovation Days 2011.
- [20] Jiang, Y., Zeng, L., & Luo, Y. (2013). Multiobjective gate assignment based on passenger walking distance and fairness. *Mathematical Problems in Engineering*, 2013. <https://doi.org/10.1155/2013/361031>
- [21] Deng, W., Zhao, H., Yang, X., Li, D., Li, Y., & Liu, J. (2018). Research on a robust multi-objective optimization model of gate assignment for hub airport. *Transportation Letters*, **10**(4), pp. 229–241.
- [22] Pilon, N., Cook, A.J., Ruiz, S., Bujor, A., & Castelli, L. (2016). Improved flexibility and equity for airspace users during demand-capacity imbalance—an introduction to the user-driven prioritisation process. Sixth SESAR Innovation Days.
- [23] Hu, X., Teng, J., Wu, W., Li, Y., & Sheng, Y. (2021). Research on airport scheduling of FGAP multi-objective programming model based on uncertainty theory. *Symmetry*, **13**(10), 1915. <https://doi.org/10.3390/sym13101915>
- [24] SAA-State Airports Authority (2021) – STAR Chart (LTFJ RWY 06) – Published by SAA, Turkey.
- [25] Kasimbeyli, R., Ozturk, Z.K., Kasimbeyli, N., Yalcin, G.D., & Erdem, B.I. (2019). Comparison of some scalarization methods in multiobjective optimization: comparison of scalarization methods. *Bulletin of the Malaysian Mathematical Sciences Society*, **42**, pp. 1875–1905.
- [26] ICAO. (2018), “ICAO Doc 8168 – Aircraft operations-Flight Procedures”, 6th edition, Canada.
- [27] ICAO. (2020), “ICAO Doc 9889 - Airport air quality manual”, 2nd edition, Canada.
- [28] ICAO. (2021), “ICAO aircraft engine emissions databank”, Available at: www.easa.europa.eu/domains/environment/icao-aircraft-engine-emissions-databank
- [29] Leech, N., Barrett, K., & Morgan, G.A. (2013). *SPSS for intermediate statistics: Use and interpretation*. Routledge.
- [30] Büyüköztürk, S. (2007). Sosyal Bilimler için Veri Analizi El Kitabı (En: Data Analysis Handbook for Social Science). Ankara: Pegem Akademi Yayıncılık (En: Pegem Akademi Publishing).